Changes in brain connectivity linked to multisensory processing of pain modulation in migraine with acupuncture treatment

Lu Liu [a,1], Tian-Li Lyu [a,1], Ming-Yang Fu [b,1], Lin-Peng Wang [a], Ying Chen [a], Jia-Hui Hong [a], Qiu-Yi Chen [a], Yu-Pu Zhu [c], Zhong-Jian Tan [d], Da-Peng Liu [e], Zi-Wei Chen [b,*], Ya-Zhuo Kong [c,*], Bin Li [a,*]

[a] *Department of Acupuncture and Moxibustion, Beijing Hospital of Traditional Chinese Medicine, Capital Medical University, Beijing Key Laboratory of Acupuncture Neuromodulation, Beijing 100010, China*
[b] *School of Electronic and Information Engineering, Beijing Jiaotong University, Beijing 100044, China*
[c] *Department of Psychology, University of Chinese Academy of Sciences, Beijing 100049, China*
[d] *Department of Radiology, Dong Zhimen Hospital Beijing University of Chinese Medicine, Beijing 100700, China*
[e] *Beijing University of Chinese Medicine Third Affiliated Hospital, Beijing 100029,China*

ARTICLE INFO

ABSTRACT

Migraine without aura (MWoA) is a major neurological disorder with unsatisfactory adherence to current medications. Acupuncture has emerged as a promising method for treating MWoA. However, the brain mechanism underlying acupuncture is yet unclear. The present study aimed to examine the effects of acupuncture in regulating brain connectivity of the key regions in pain modulation. In this study, MWoA patients were recruited and randomly assigned to 4 weeks of real or sham acupuncture. Resting-state functional magnetic resonance imaging (fMRI) data were collected before and after the treatment. A modern neuroimaging literature *meta*-analysis of 515 fMRI studies was conducted to identify pain modulation-related key regions as regions of interest (ROIs). Seed-to-voxel resting state-functional connectivity (rsFC) method and repeated-measures two-way analysis of variance were conducted to determine the interaction effects between the two groups and time (baseline and post-treatment). The changes in rsFC were evaluated between baseline and post-treatment in real and sham acupuncture groups, respectively. Clinical data at baseline and post-treatment were also recorded in order to determine between-group differences in clinical outcomes as well as correlations between rsFC changes and clinical effects. 40 subjects were involved in the final analysis. The current study demonstrated significant improvement in real acupuncture *vs* sham acupuncture on headache severity (monthly migraine days), headache impact (6-item Headache Impact Test), and health-related quality of life (Migraine-Specific Quality of Life Questionnaire). Five pain modulation-related key regions, including the right amygdala (AMYG), left insula (INS), left medial orbital superior frontal gyrus (PFCventmed), left middle occipital gyrus (MOG), and right middle cingulate cortex (MCC), were selected based on the *meta*-analysis on brain imaging studies. This study found that 1) after acupuncture treatment, migraine patients of the real acupuncture group showed significantly enhanced connectivity in the right AMYG/MCC-left MTG and the right MCC-right superior temporal gyrus (STG)

compared to that of the sham acupuncture group; 2) negative correlations were established between clinical effects and increased rsFC in the right AMYG/MCC-left MTG; 3) baseline right AMYG-left MTG rsFC predicts monthly migraine days reduction after treatment. The current results suggested that acupuncture may concurrently regulate the rsFC of two pain modulation regions in the AMYG and MCC. MTG and STG may be the key nodes linked to multisensory processing of pain modulation in migraine with acupuncture treatment. These findings highlighted the potential of acupuncture for migraine management and the mechanisms underlying the modulation effects.

1. Introduction

Migraine without aura (MWoA) is a serious neurological disorder characterized by recurrent headaches and various autonomic nervous system dysfunctions, including nausea, photophobia, and phonophobia (2018c; Ashina et al., 2021b). This chronic and often lifelong disease affects about 1.33 billion people worldwide across diverse cultures and socioeconomic statuses (2018b). A 1-year global prevalence is estimated at 15 %: highest in southeast Asia (25–35 %) and lowest in China (9 %) (2018a). It is the second most disabling neurological disease in the global burden of nervous system diseases survey (2019). Hitherto, migraine is known as more than simply a headache, and we must consider that patients experience various accompanying symptoms in response to multisensory inputs. Clinically, it has been hypothesized that MWoA patients with sensory-related perceptive disorders have a reduced sensitivity threshold to visual, auditory, and pain stimuli and a low pre-activation level of the sensory cortex. Previous functional magnetic resonance imaging (fMRI) studies have shown that aberrant connectivity within pain and other sensory networks contributed to the progression of migraine during or between episodes (Lee et al., 2019; Ruscheweyh et al., 2019).

Adherence to the current medication for MWoA is often unsatisfactory. Due to poor tolerance to medication, some patients suffer unpleasant side effects and lack efficacy (Hepp et al., 2015). Furthermore, frequent use of medications is associated with the risk of medication overuse-induced headache (Ashina et al., 2021a). Confronted with migraine, patients with an inter-individual difference in drug response or those who are unwilling to accept possible drug-induced adverse events need an effective alternative therapy with fewer side effects is an urgent requisite.

Accumulating evidence has endorsed the potential of acupuncture treatment for MWoA (Li et al., 2012; Wang et al., 2011; Xu et al., 2020; Zhao et al., 2017). A *meta*-analysis from The Cochrane Collaboration reported that acupuncture might have an effect similar to preventive medications (Linde et al., 2016). Based on these findings, the latest consensus statement from the European Headache Federation and the European Academy of Neurology has recommended acupuncture as a stand-alone preventive treatment when medication is contraindicated (Eigenbrodt et al., 2021). Nonetheless, the neural mechanism underlying the acupuncture treatment for MWoA is unclear, which has hindered the development and incorporation of this promising treatment into mainstream medicine.

Advances in neuroimaging techniques have provided new insights into migraine pathophysiology and finding imaging markers of migraine mechanisms. Resting-state fMRI (rs-fMRI) has been commonly applied to investigate the functional organization of specific brain regions and networks responsible for pain-related processing (Schwedt et al., 2015b). A systematic review of resting-state functional connectivity (rsFC) studies in migraine (Skorobogatykh et al., 2019) has summarized that aberrant FC was found within or with a number of key regions or different networks: amygdala, insula, orbitofrontal and prefrontal cortex, occipital lobe, cingulate cortex, thalamus, hypothalamus, periaqueductal gray network, central executive network, salience network, default mode network, visual network, fronto-parietal network, and dorsal attention network. All the key regions with abnormal connectivity to those mentioned above can be categorized as pain-related

processes, including sensory-discriminative, affective emotional, cognitive, and pain modulation.

Functional neuroimaging studies supported the central modulating effects of acupuncture in normalizing altered FC within subcortical brain regions and networks as well. After long-term acupuncture, migraine patients showed increased FC mostly in or within the amygdala, insula, thalamus, precuneus, cingulate gyrus, fronto-parietal network, and default mode network, which mostly correlated with the altered areas above and were involved in the processing of nociceptive information and emotion (Chang et al., 2021; Tian et al., 2021). Additionally, a few researchers recently reported decreased FC in other areas including the amygdala, insula, thalamus, superior frontal gyrus, and postcentral gyrus (Tian et al., 2021; Wei et al., 2022). The mechanism of acupuncture efficacy for migraine may be related to the regulation of pain-related brain network, however, the specific way of acupuncture modulation under the heterogeneity of fMRI results remains for further discussion (Liu et al., 2021).

The *meta*-analysis database of Neurosynth is an open-source platform for large-scale, automated synthesis of fMRI data extracted from published articles (1334 terms in 14,371 studies, as of March 2022) (Yarkoni et al., 2011). Neurosynth is a brain mapping framework that incorporates text-mining, *meta*-analysis, and machine-learning techniques to generate a large database of mappings. This approach can be used to automatically conduct large-scale, high-quality neuroimaging *meta*-analyses that address long-standing inferential problems in the neuroimaging literature. Previous methods have relied heavily on manual efforts or specific domains, which might have limited the scope and efficiency of the resulting analyses (Yarkoni et al., 2011). In the seed-based FC studies, the regions of interest (ROIs) are usually derived from previous functional studies and require prior knowledge of seeds (Cole et al., 2010). Contrary to the previous hypothesis-driven ROI selection approach, we first applied Neurosynth *meta*-analysis to identify pain modulation-related key regions.

This study conducted a *meta*-analysis to identify the pain modulation-related key regions as ROIs. Then, a seed-to-voxel rsFC analysis was made on MWoA patients to identify the potential brain regions functionally correlated with these pain modulation-related key regions in order to investigate the modulation mechanisms underlying acupuncture treatment.

2. Methods

The study was approved by the Ethics Committees of Beijing Hospital of Traditional Chinese Medicine, Capital Medical University in Beijing, China (No. 2016BL-081-02). All patients were required to provide written informed consent before participation in this study that was conducted following the principles of the Declaration of Helsinki (2013b).

2.1. Participants

The study was conducted in the outpatient departments of Beijing Hospital of Traditional Chinese Medicine, Capital Medical University. The patients were recruited via a multimodal strategy, including hospital social media (WeChat), website, newspaper, patient databases, and community service center posters. A neurologist assessed the eligibility

of all potential patients following pre-defined inclusion/exclusion criteria and explained to them the study design. Finally, patients with MWoA (n = 64) were enrolled in this study.

The inclusion criteria were as follows: (1) age18–65 years; (2) meeting the diagnostic criteria according to the International Classification of Headache Disorders, 3rd edition β version (2013a) (versions III beta) for MWoA; (3) having at least two migraine attacks in the last 4 weeks; (4) a history of migraine for at least 1 year; (5) not received prophylactic treatments using acupuncture or pharmacological medicine in the past 3 months; (6) were able to complete the headache diary; (7) provided written informed consent.

The exclusion criteria were as follows: (1) tension-type headache, cluster headache, or other primary headaches; (2) secondary headache caused by otorhinolaryngology diseases or intracranial pathological changes; (3) medication overuse headache; (4) severe systemic diseases (such as angiocardiopathy, cerebrovascular disease, hepatopathy, nephropathy, acute infectious disease, hematopathy, endocrinopathy, allergy, or methysis); (5) pregnancy, lactation, or insufficient contraception; (6) psychiatric or neurological disorders (for example, major depressive disorder (MDD), schizophrenia, bipolar disorder, traumatic brain injury, stroke, Parkinson's disease); (7) MRI contraindications (claustrophobia, cardiac pacemaker, or other metallic agents embedded within the body); (8) use of opioids analgesics.

2.2. Experimental procedures

Patients were randomized into two groups using a permuted block randomization (block length was 4): real acupuncture or sham acupuncture. Patients received treatment in specific acupuncture rooms with compartments to avoid communication between the two groups. Hence, the participants were blinded to their group allocation. The acupuncturist was not blinded to treatment allocation due to different interventions; however, the acupuncturist was not allowed to discuss the type of intervention. Furthermore, outcome assessors, the fMRI scanner,

and statisticians were blinded to group allocation throughout the trial. The study design is illustrated in Fig. 1a.

An independent assistant separated and opened each opaque and sealed envelope in the sequence corresponding to the screening order and assigned the eligible patients. The treatment allocation results were forwarded to the acupuncturist by this assistant.

2.3. Acupuncture treatment

To ensure treatment consistency, one acupuncturist attended special training on the procedure of this study before recruitment and then delivered the standard treatment. This acupuncturist was licensed as a practicing physician, registered with the Ministry of Health of the People's Republic of China, and had clinical experience for >20 years. All patients underwent twelve sessions of acupuncture in 4 weeks, with three sessions/week. In both the real and sham acupuncture groups, the acupuncture treatment began after randomization. The details of acupuncture (location of real acupoints/sham acupoints and depth of insertion) are shown in Table S1.

Patients in the real acupuncture treatment group received manual acupuncture at eight obligatory real acupoints, including bilateral Fengchi (GB20), Fengfu (GV16), Baihui (GV20), bilateral Taiyang (EX-HN5), and bilateral Hegu (LI4) (Fig. 1b, Table S1) with disposable single-use sterile needles (0.25×25 mm, Huatuo Medical Instrument Co., ltd, Suzhou, China). The standardized acupuncture protocol had been proven effective based on a consensus meeting with clinical experts and our previous clinical trial (Wang et al., 2011). The positions of the acupoints were according to the standards issued by the World Health Organization (WHO) in 2010 (Region, 2010). After skin disinfection using alcohol, needles were inserted into the acupoints at 10–15 mm depth. The acupuncturist twisted the needles bi-directionally by 90°–180°, lifting and thrusting needles with an amplitude of 3–5 mm to induce de-qi sensation (including soreness, numbness, distention, and heaviness). After the de-qi sensation was attained, the needles were
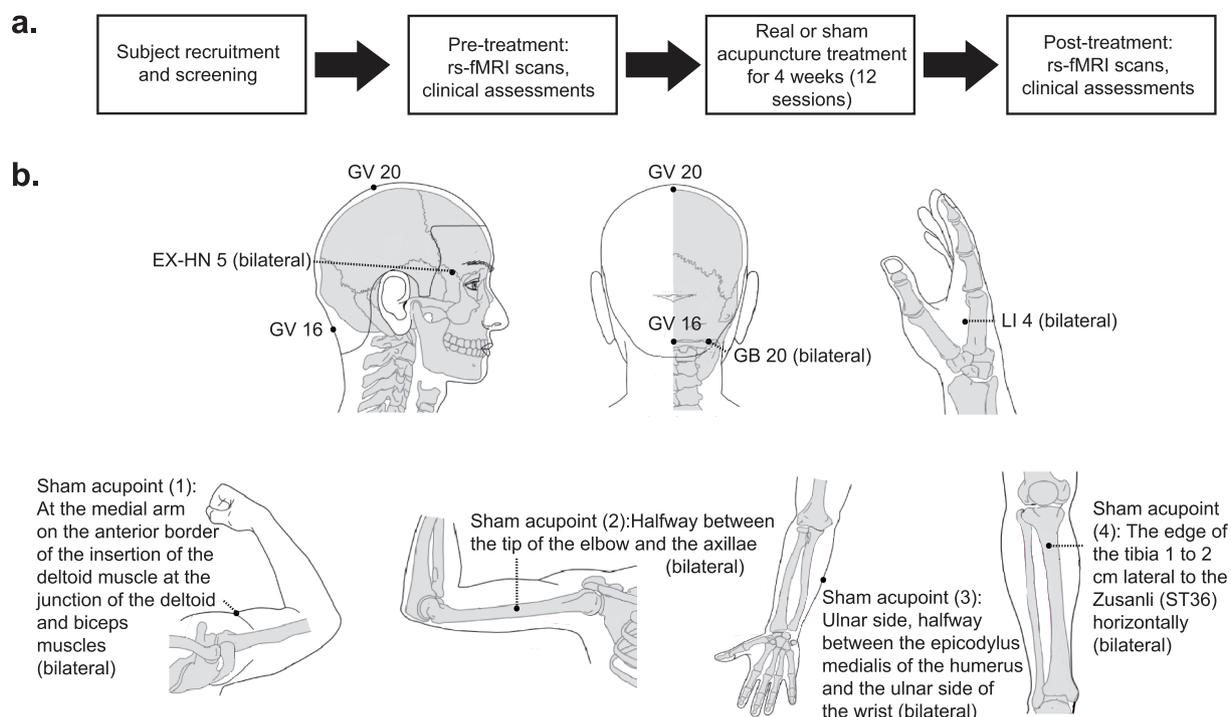
Fig. 1. Study overview. **(a)** The procedure for the study including subject recruitment and screening, pre-treatment (resting-state fMRI scans, clinical assessments), real or sham acupuncture treatment 4 weeks and post-treatment (resting-state fMRI scans, clinical assessments). **(b)** The location of real acupoints and sham acupoints. Real acupoints (bilateral EX-HN 5, bilateral GB 20, bilateral LI 4, GV 20 and GV 16). Sham acupoints (superficial skin penetration treatment over non-acupoints). Abbreviations: EX-HN 5, Taiyang (Extra point head and neck 5); GV 20, Baihui (Governor 20); GV 16, Fengfu (Governor 16); GB 20, Fengchi (Gallbladder 20); LI 4, Hegu (Large intestine 4).

retained at the acupoints for 30 min. During the 30 min, the above procedures will be manipulated for 10 s every 10 min to maintain the de-qi sensation.

Patients in the sham acupuncture control group received a superficial skin penetration treatment at the eight sham acupoints. To minimize the physiological effects, these sham acupoints did not belong to any known meridian and were not conventional acupoints according to previous studies (Li et al., 2009; Li et al., 2012) (Fig. 1b, Table S1). Superficial skin penetration at sham acupoints without needle manipulation for de-qi sensation is a common sham acupuncture method used in previous randomized controlled trials (Zhao et al., 2017). Patients in this group underwent an acupuncture procedure similar to that in the real acupuncture treatment group. In addition, sterile steel needles of the same size and number for each treatment session were identical to those used in the real acupuncture treatment group.

Patients were not allowed to take any prophylactic medications. In case of severe pain (visual analog score (VAS) >8), ibuprofen (300 mg capsules with sustained-release) was allowed as the only rescue medication, and the usage was documented in the headache diary. All patients were instructed not to take any other analgesics except for ibuprofen.

2.4. Clinical outcomes and data analysis

2.4.1. Headache severity: Monthly migraine days (MMDs) and VAS

The headache severity outcome measures include (1) change in MMDs from baseline to week 4; (2) change in VAS from baseline to week 4. Similar to a previous study of acupuncture intervention on migraine (Xu et al., 2020), we chose MMDs as the primary outcome.

Independent research assistants supervised the patients to complete their headache diaries in paper and pencil format from baseline to week 4 and evaluated the outcomes. In the headache diaries (Russell et al., 1992), the participants recorded the details of their migraine attacks, including attack frequency, duration, and days, the characteristic and intensity of pain (VAS 0–10), locations, inducements of the headache, concomitant symptoms (nausea, vomiting, photophobia, and phonophobia), aggravation by routine physical activity, precipitating factors, and acute medications (if any) taken for each migraine attack.

2.4.2. Headache impact: Headache impact Test-6 (HIT-6)

HIT-6 is a short, self-administered questionnaire developed as a global measure of adverse headache impact using widely measured, functionally relevant domains: pain, social and role limitations, cognitive functioning, vitality, and psychological distress (Dowson, 2001; Kosinski et al., 2003). The six questions are scored 6, 8, 10, 11, or 13 points based on the five response categories that assess how often the headaches interfere with activities or cause distress (never, rarely, sometimes, very often, or always). The scores for all glossary-six items are summed to produce a total HIT-6 score (range: 36–78), interpreted as little or no impact (≤49), some impact (50–55), substantial impact (56–59), and severe impact (60–78) due to headache with higher scores indicating greater impact and decreased scores consistent with improvement.

2.4.3. Health-related quality of life (HRQoL): migraine-specific quality of life questionnaire (MSQ)

MSQ is a self-administered, migraine-specific, 14-item instrument assessment of the HRQoL across three domains that was developed to assess the effect of migraine on daily functions (Jhingran et al., 1998a; Jhingran et al., 1998b). The role restrictive (MSQ-RR) domain measures the effect of migraine on daily social and work-related activities, the role preventive (MSQ-RP) domain assesses whether migraine prevents the individual from performing these activities, and the emotional functioning (MSQ-EF) domain measures the emotions associated with migraine. Items are rated on a six-point scale (none of the time, a little bit of the time, some of the time, a good bit of the time, most of the time,

and all of the time). The raw domain scores are summed and transformed to a 100-point scale, with higher scores indicating a better QoL and improvement.

2.4.4. Psychological profile: Beck depression Scale-II (BDI-II) and Beck anxiety scale (BAI)

BDI-II is a self-reported questionnaire to evaluate the severity of depression (Beck et al., 1996a; Beck et al., 1996b; Steer et al., 1999). It consists of 21 symptoms related to MDD diagnostic criteria in the fourth edition of the Diagnostic and Statistical Manual of Mental Disorders (DSM-IV) (Frances et al., 1995). Each symptom is graded on a four-point Likert scale (0–3), and the total score range was 0–63. Higher scores indicated higher levels of depression.

BAI was published in the USA by A. T. Beck in 1988 and is an anxiety measure that has been carefully designed to avoid confusion with depression (Beck et al., 1988). BAI consists of 21 self-reported items highlighting somatic, affective, and cognitive signs of anxiety symptoms. Each item has four possible answers with scores from 0 to 3: 0 = Not at all; 1 = Mild, but it did not bother me much; 2 = Moderate, it was not pleasant at times; 3 = Severe, it bothered me a lot. The total score was 63 points.

2.4.5. Sleep quality: Pittsburgh sleep quality Index (PSQI)

PSQI is a self-rated questionnaire that organically combines the quality and quantity of sleep to evaluate the sleep status of the subjects in the last month. PSQI scale is often used to evaluate the impact of migraine on sleep quality (Stanyer et al., 2021). A total of 19 items generated seven measures, including subjective sleep quality, sleep latency, sleep duration, habitual sleep efficiency, sleep disturbances, use of sleeping medication, and daytime dysfunction (Buysse et al., 1989). Each indicator is scored on a scale of 0–3. The sum of the scores of these seven components produces a PSQI total score. The global PSQI score ranges from 0 to 21, with high scores indicating poor sleep quality. PSQI score >5 differentiates between good and poor sleepers with 89.6 % sensitivity and 86.5 % specificity (Singh et al., 2020).

2.4.6. Cognitive function: Montreal cognitive assessment (MoCA)

MoCA is an assessment tool for rapid screening of cognitive dysfunction. Herein, 11 items were examined in eight cognitive areas: attention and concentration, executive function, memory, language, visual structure skills, abstract thinking, computation, and orientation. The total score was 30: ≥ 26 is considered normal. The higher the score, the better the cognitive level (Nasreddine et al., 2005). Recent studies have shown that some migraineurs suffer from cognitive deficits. Although it cannot be used as a diagnostic tool, MCoA screens the cognitive status of migraineurs (Santangelo et al., 2016) with high sensitivity and short test time, making it suitable for clinical application. Nonetheless, it is affected by various factors, including education level, cultural background, examination environment, and emotional and mental state of the subjects, rendering it rather sensitive to the screening of mild cognitive impairment (Nasreddine et al., 2005; O'Driscoll and Shaikh, 2017).

The above clinical outcome measures were repeatedly assessed at baseline and week 4 by an independent research assistant blinded to group allocation to ensure consistency. The same research assistant would perform the neuropsychological tests before and after treatment in a quiet room for all participants who met the inclusion criteria.

2.4.7. Clinical data analysis

All analyses were performed using Statistical Package for Social Science (SPSS) for Windows (V.25) (International Business Machines IBM, Chicago, IL, USA) by statisticians blinded to the entire allocation and intervention process. The histograms and normal probability plots were analyzed, and a Shapiro-Wilk test was conducted to determine whether the data followed a normal distribution. The means, standard deviations (SDs), and 95 % confidence intervals (CIs) were calculated.

Two-tailed analyses were conducted, with the level of statistical significance defined as *p*-value < 0.05.

The continuous variables were presented as the mean with SD or median and interquartile range, and the categorical variables were presented as numbers and percentages. For the demographic and clinical information at baseline, the chi-square test or Fisher's exact test was used to compare the dichotomous data. The independent two-sample *t*-test was used for normally distributed continuous data and the Wilcoxon rank-sum test for non-normally distributed data. The pre- and post-treatment change score between groups was compared using an independent two-sample *t*-test.

2.5. Identifying pain modulation-related brain regions from meta-analysis

Neurosynth database (https://neurosynth.org/) is a platform for large-scale, automated synthesis of fMRI data. This approach automatically extracts the activation coordinates to conduct a comprehensive automated *meta*-analysis for several hundred terms of interest. A high-frequency term within the article text is identified for each term, and all the associated activation foci were submitted to a *meta*-analysis (Yarkoni et al., 2011). To delineate the brain regions corresponding to pain modulation-related brain regions on the cerebrum, we first used Neurosynth for *meta*-analysis using the search term "pain." This *meta*-analysis extracted 515 fMRI studies from December 1998 to February 2018 (Table S2). Neurosynth provides two types of statistical inference maps: uniformity and association tests. While uniformity test maps provide information about the consistency of activation for a specific process, the association test maps provide information about the relative selectivity that activates the regions in a specific process. Since the present study aimed to investigate pain modulation-related neuroimaging change in acupuncture on the cerebrum rather than providing information on a specific given process, we chose the "uniformity test" map (Fig. S1). A false-discovery rate (FDR) adjusted *p*-value of 0.01 was applied to produce the uniformity test map. Next, five pain modulation-related ROI coordinates with peak z-scores were selected within all clusters >95 voxels by xjView toolbox V.8 (https://www.alivelearn.net/xjview/). Then, MarsBaR toolbox (https://sourceforge.net/projects/marsbar/) was utilized to generate five spherical ROIs with a 6-mm radius and a mask of all ROIs for subsequent analysis (Fig. S2). Finally, these brain ROIs were refined by taking the overlap of the masks and the original uniformity test map, including the right amygdala (AMYG) for ROI-1, left insula (INS) for ROI-2, left medial orbital superior frontal gyrus (PFCventmed) for ROI-3, left middle occipital gyrus (MOG) for ROI-4, and right middle cingulate cortex (MCC) for ROI-5.

2.6. fMRI data acquisition

The MRI scans were conducted before and after 4 weeks of real or sham acupuncture intervention. The rs-MRI data were obtained with a 3.0 Tesla superconductor (Siemens Magnetom Verio, Erlangen, Germany) at Dong Zhimen Hospital Beijing University of Chinese Medicine. All subjects underwent MRI scanning during the headache-free interval (not within 48 h after the last migraine attack).

The whole-brain functional images were recorded using a T2*-weighted gradient echo echo-planar imaging sequence blood oxygenation level-dependent (BOLD) pulse sequence (time repetition (TR)/time echo (TE) = 2420/30 ms, slice thickness = 3.0 mm, slice number = 44, volume number: 300, voxel size = $3.0 \times 3.0 \times 3.0$ mm^3, field of view (FOV) = 192×192 mm^2, flip angle (FA) = 90°, matrix size = 64×64) to obtain fMRI data.

High-resolution whole-brain structural images were recorded using a T1-weighted isotropic multi-echo magnetization-prepared rapid acquisition gradient-echo (MPRAGE) pulse sequence (TR/TE = 2000/3.51 ms, slice thickness = 1.00 mm, slice number = 192, voxel size: $1 \times 1 \times 1$ mm^3, FOV = 256×256 mm^2, FA = 8°, matrix size = 256×256) for anatomic localization of significant signal changes.

The subjects were required to lie in a supine position during the scanning. To avoid head motions from disturbing the image, a headrest was utilized to hold the head, and a 16-channel radio-frequency head coil was fixed on both sides of the headrest. All participants were instructed to stay awake, relax, keep their eyes open, blink normally when staring at centrally positioned fixation cross (+), and not think about anything particular during the whole scan with their ears plugged to attenuate the gradient noise. A radiologist reviewed all scans qualitatively to check for probable brain lesions or structural abnormalities.

2.7. Image preprocessing

We employed the ROIs obtained in the *meta*-analysis to perform a seed-to-voxel FC analysis using rs-fMRI data from migraineurs (Fig. 2). The fMRI images were first preprocessed using CONN V.20b (https://www.nitrc.org/projects/conn) in MATLAB (R2016b V.9.1; Mathworks, Nantick, MA, USA). During the preprocessing part, the image underwent Conn's default preprocessing pipeline steps as follows, realignment and unwrap, slice-timing correction, Artifact Repair Toolbox (ART)-based (https://www.nitrc.org/projects/artifact_detect/) outlier detection (>3 SD and >0.5 mm) for scrubbing regression, direct segmentation for gray and white matter and cerebrospinal fluid (CSF) and normalization to the T1-weighted MNI152 template, functional smoothing with $6 \times 6 \times 6$ mm^3 full-width at half-maximum (FWHM) Gaussian kernel, and a band-pass filter of 0.01–0.1 Hz during the BOLD response. Then, voxel-wise brain rsFC analysis was performed with the residual fMRI signal of the involved participants.

2.8. FC calculation and analysis

Data Processing and Analysis for Brain Imaging (DPABI) V.5.2 (https://rfmri.org/dpabi) was used for the whole-brain FC calculation. First, we extracted a mean BOLD signal within the seeds as described above (right AMYG, left INS, left PFCventmed, left MOG, right MCC, and a mask of all ROIs) and calculated the Pearson's correlation coefficients with the rest of the whole brain for each subject. Fisher-Z-transformation was applied to all correlation values to improve the normality. The FC maps from each subject were then utilized for group-level analysis. To explore the interaction effects between groups (real and sham acupuncture) and times (pre- and post-treatment), we conducted a repeated-measures two-way analysis of variance (ANOVA) using the Statistical Parametric Mapping (SPM) 12 (http://www.fil.ion.ucl.ac.uk/spm/), with age, sex, and educational years as covariates; the surviving brain clusters were chosen as ROIs for the post-hoc analysis: A two-tailed two-sample *t*-test was applied on these interaction effect ROIs to determine the difference between groups at baseline and post-treatment, with respect to age, sex and educational years as covariates.

A paired *t*-test was applied to explore the FC change before and after treatment in both groups with respect to age, sex, and educational years as covariates. For multiple comparisons, the results were further corrected with Gaussian random field (GRF) approach (voxel-level P < 0.001, cluster-level P < 0.05) in the DPABI toolbox, and cluster >10 voxels were reported.

2.9. Correlations analysis

The correlations between the rsFC z-score change and clinical features (including monthly migraine days, VAS, MSQ, HIT-6, BDI-II, BAI, PSQI, and MoCA) were evaluated by statistical analyses using SPSS (V.25). Shapiro–Wilks test was used to check the normality of the data. The average z-score values of the significantly altered rsFC seeds pre- and post-acupuncture intervention were extracted. Next, Pearson's correlation analysis determined the associations between the rsFC change and clinical features. Bonferroni corrections were used for multiple comparisons. Both uncorrected P value and Bonferroni-corrected P value were reported. In order to predict the effects on the
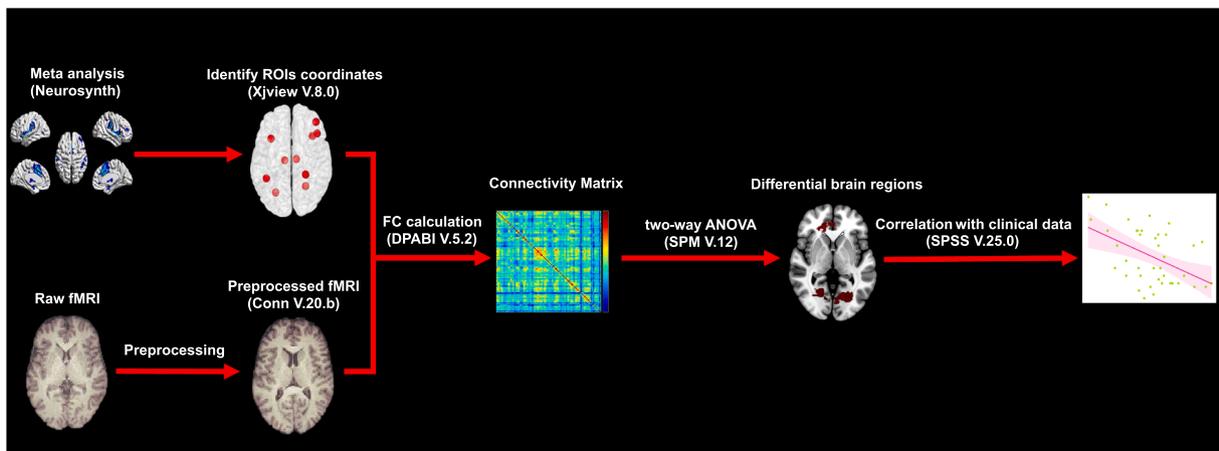
Fig. 2. Flow chart of resting-state fMRI data processing and analysis. Step 1: Extract "uniformity test map" of pian from Neurosynth and identify ROI coordinates with Xjview V. 8.0. Step 2: resting state fMRI data preprocessing of migraine without aura patients with Conn V. 20b. Step 3: Extract a mean BOLD signal within the ROIs and calculated Pearson's correlation coefficients with the rest of the whole brain for each subject with DPABI V. 5.2. Step 4: Conduct a two-way ANOVA analysis on the Fisher transformed maps to investigate the differences in rsFC between the real and sham acupuncture group with SPM V. 12. Step 5: Compute the correlation between the rsFC z-score changes and clinical characteristics with SPSS V. 25. Abbreviations: ROI, region of interest; BOLD, Blood oxygenation level dependent; fMRI, functional magnetic resonance imaging; rsFC,resting state functional connectivity.
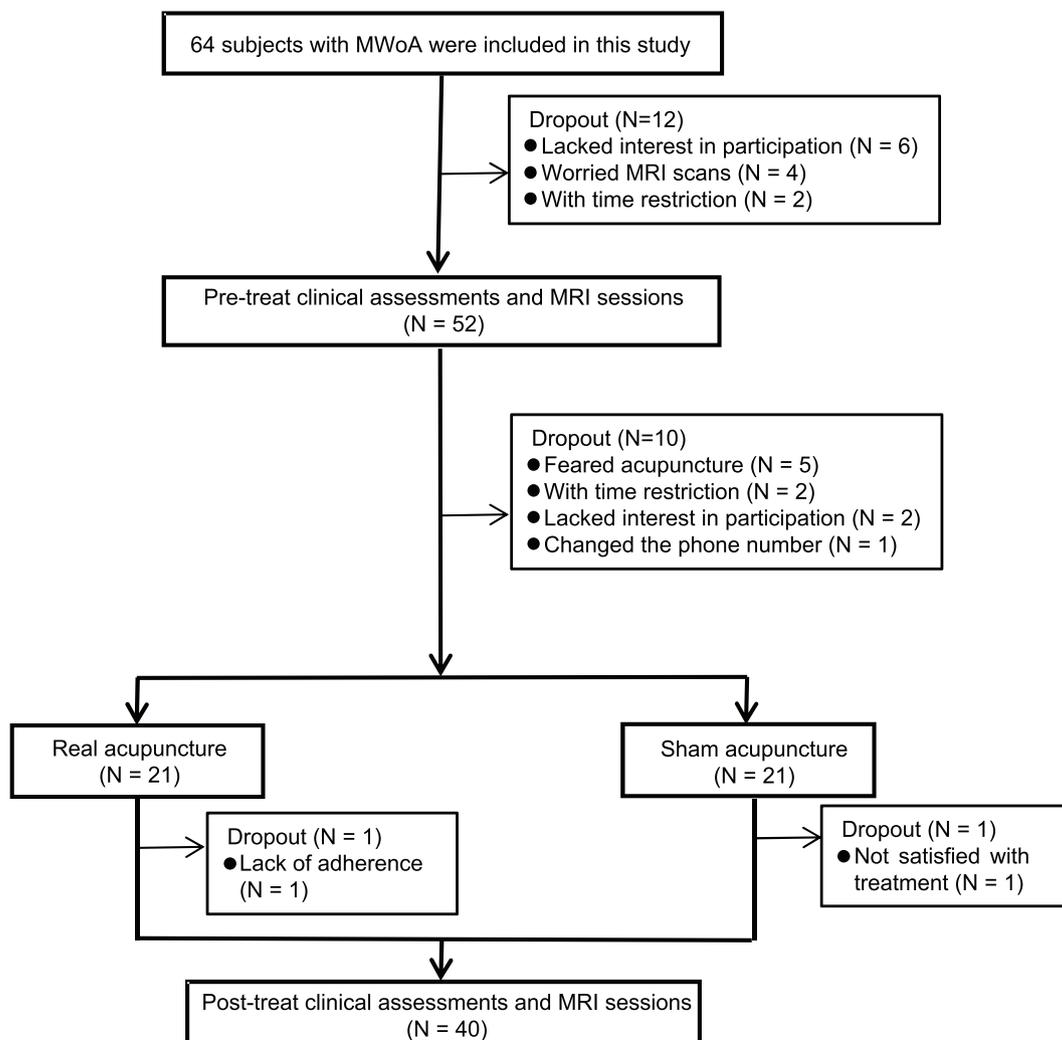
Fig. 3. Procedures and data used for the study.

clinical outcomes of acupuncture, a hierarchical multiple regression analysis was applied to test the association between the average z-score values of the surviving brain clusters' rsFC at baseline and the altered MMDs, with age, sex, and educational years as covariates. The significance threshold was set at P < 0.05.

3. Results

3.1. Participants and baseline demographics

A total of 64 patients with MWoA were included in this study. Of these, 12 dropped out of the study before the baseline MRI sessions (lacked interest in participation n = 6, worried about MRI scans n = 4, had time constraints n = 2), and 10 dropped out before the first acupuncture treatment (feared acupuncture n = 5, had time constraint n = 2, lacked interest in participation n = 2, changed the phone number n = 1). Then, 42 subjects were treated with real or sham acupuncture for 4 weeks (Table S3). Two patients did not complete their treatment (real acupuncture group: lack of adherence n = 1; sham acupuncture group: not satisfied with treatment n = 1). Finally, 40 subjects were involved in the final analysis (Fig. 3).

Baseline demographics did not differ significantly between the real and sham acupuncture groups (all P > 0.05) (Table 1). At baseline, the mean age of the patients was 37 years, and the mean duration of migraine diagnosis was 15 years. The majority of patients (90 %) were females. Amongst 4 participants in the real acupuncture group belong to chronic migraine, 6 participants in the sham acupuncture group belong to chronic migraine. Non-steroidal anti-inflammatory drugs (NSAIDs) were the most commonly used drug, neither combination analgesics, opioids nor antiemetics were found to be taken in either group.

3.2. Clinical outcomes results

3.2.1. Headache severity: MMDs

The treatment groups' baseline MMDs were similar (real acupuncture 4.78 ± 2.45 *vs* sham acupuncture 5.17 ± 2.77; P = 0.64). The decrease MMDs from baseline was significantly larger in the real acupuncture group than in the sham acupuncture group over the treatment phase, with a between-group difference of 1.63 (95 % confidence interval (CI): 0.01–3.24; P = 0.0485) days during the treatment phase (Table 2).

3.2.2. Headache impact: HIT-6 results

At baseline, the mean HIT-6 score was comparable between the treatment groups (real acupuncture 70.80 ± 5.18) *vs* sham acupuncture 68.50 ± 5.62; P = 0.19) (Table 2). All patients were seriously affected by the migraine attacks, with 100 % having a total HIT-6 score of 60 (severe headache impact).

The changes in HIT-6 scores were significantly larger in the real acupuncture group than in the sham acupuncture group, with a between-group difference of 8.40 (95 % CI:4.47–12.33; *p* = 0.0001) scores during the treatment phase (Table 2). The between-group HIT-6 minimally important difference (MID) (≥2.3 points) (Coeytaux et al., 2006) was achieved after the acupuncture treatment.

3.2.3. HRQoL: MSQ scores

The treatment groups' baseline mean MSQ domain scores were similar (RR: real acupuncture 53.71 ± 18.83 *vs* sham acupuncture 42.13 ± 21.06), P = 0.07; RP: real acupuncture 64.00 ± 17.37) *vs* sham acupuncture 54.70 ± 25.28), P = 0.18; EF: real acupuncture 64.00 ± 27.05) *vs* sham acupuncture 41.29 ± 26.44), P = 0.23), and all domains' mean scores were ≤ 64 points (Table 2), suggesting poor HRQoL.

At the end of the treatment phase, significant between-group differences were detected in MSQ-RR and MSQ-RP domains (RR: P = 0.0470; RP: P = 0.0280) in favor of real acupuncture, reflecting improved HRQoL (Table 2). The between-group difference was greater

Table 1

Demographics and baseline characteristics of migraine without aura patients.

Characteristics	Real Acupuncture group n = 20	Sham Acupuncture group n = 20	Total n = 40	P value[a]
Age – year				
Mean (SD)[b]	38.60 (12.27)	36.10 (9.61)	37.35 (10.95)	0.5435
Median (IQR)	36.00 (31.00–45.00)	33.00 (30.00–38.25)	33.00 (31.00–42.00)	
Range	18.00–60.00	27.00–59.00	18.00–60.00	
Sex – no. (%)				
Female[c]	17 (85.00)	19 (95.00)	36 (90.00)	0.6050
Male[c]	3 (15.00)	1 (5.00)	4 (10.00)	
Education-year				
Mean (SD)[b]	15.65 (2.50)	15.15 (3.05)	15.40 (2.76)	0.5738
Marriage – no. (%)				
Married/single[c]	3 (15.00)/17 (85.00)	6 (30.00)/14 (70.00)	9 (22.50)/31 (77.50)	0.4489
Duration of migraine diagnosis at baseline – year, mean (SD)	16.30 (10.79)	14.50 (7.04)	15.40 (9.04)	0.5357
Chronic migraine[c,d] – no. (%)	4 (20.00)	6 (30.00)	10 (25.00)	0.4652
Use of acute pain medication – no (%)				
NSAIDs[c]	5 (25.00)	6 (30.00)	11 (27.50)	0.7233
Combination analgesics[c]	0	0	0	
Opioids[c]	0	0	0	
Ergots[c]	1 (5.00)	1 (5.00)	2(15.00)	
Triptans[c]	0	1 (5.00)	1 (5.00)	
Antiemetics[c]	0	0	0	
Days of acute medication use per month				
Median (IQR)	2.00 (1.50–3.00)	2.33 (1.75–3.25)	2.00 (2.00–3.00)	
Range	1.00–3.00	1.00–4.00	1.00–4.00	

Abbreviations: *SD* standard deviation; *IQR* interquartile range; *no. (%)* number; *NSAIDs* Non-steroidal anti-inflammatory drugs.

[a] All tests were two-sided. Statistical significance was set at *P* < 0.05.

[b] Analyzed using independent samples *t-test*.

[c] Analyzed using Chi-square test.

[d] According to the International Classification of Headache Disorders (versions III beta), chronic migraine meets the criteria that migraine days onset ≥ 8 days/month for 3 months, fulfilling the diagnosis of migraine without aura.

than the between-group MID in the RP domain (RP = 15.20; RP MID = 4.6) and RR domain (RR = 12.99; MID = 3.2) after the treatment phase (Cole et al., 2009).

However, no significant difference was observed in the mean VAS, BDI-II, BAI, PSQI, and MoCA between the real and sham acupuncture at week 4.

Table 2.

3.3. Rois identified from the meta-analysis

Five clusters with five coordinates were determined from the uniformity test map of Neurosynth database. To facilitate the following FC

Table 2
Clinical outcomes of migraine without aura patients between real acupuncture and sham acupuncture groups.

Outcome Measure	Real Acupuncture group n = 20	Sham Acupuncture group n = 20		Between-group difference
			Value (95 % CI)	P value[a]
MMDs, mean (SD)[b]				
Baseline	4.78 (2.45)	5.17 (2.77)		
Treatment, 1-4wk	1.23 (0.77)	3.25 (2.52)		
Change from baseline in MMDs	3.54 (2.27)	1.92 (2.76)	1.63 (0.01 to 3.24)	0.0485
Mean VAS score, mean (SD)[b]				
Baseline	7.60 (1.50)	7.50 (1.54)		
Treatment, 1-4wk	5.10 (2.10)	5.90 (1.74)		
Change from baseline in VAS	2.50 (2.35)	1.60 (1.96)	0.90 (-0.48 to 2.28)	0.1961
HIT-6, mean (SD)[b]				
Baseline	70.80 (5.18)	68.50 (5.62)		
Treatment, 1-4wk	59.45 (7.93)	65.55 (6.48)		
Change from baseline in HIT-6	11.35 (6.72)	2.95 (5.49)	8.40 (4.47 to 12.33)	0.0001
MSQ, Role restrictive domain, mean (SD)[b]				
Baseline	53.71 (18.83)	42.13 (21.06)		
Treatment, 1-4wk	76.90 (18.99)	51.50 (25.57)		
Change from baseline in MSQ-RR domain	−22.36 (20.37)	−9.37 (19.63)	−12.99 (-25.79 to −0.18)	0.0470
MSQ, Role preventive domain, mean (SD)[b]				
Baseline	64.00 (17.37)	54.70 (25.28)		
Treatment, 1-4wk	82.50 (20.99)	58.00 (26.53)		
Change from baseline in MSQ-RP domain	−18.50 (9.94)	−13.63 (22.07)	−15.20 (-28.67 to −1.73)	0.0280
MSQ, Emotional functioning domain, mean (SD)[b]				
Baseline	64.00 (27.05)	41.29 (26.44)		
Treatment, 1-4wk	83.67 (15.21)	62.83 (23.07)		
Change from baseline in MSQ-EF domain	−19.67 (24.42)	−9.17 (26.77)	−10.50 (−26.90 to 5.90)	0.2029
BDI-II, mean (SD)[b]				
Baseline	8.00 (4.57)	10.60 (7.24)		

Table 2 (*continued*)

Outcome Measure	Real Acupuncture group n = 20	Sham Acupuncture group n = 20		Between-group difference
			Value (95 % CI)	P value[a]
Treatment, 1-4wk	4.05 (4.54)	9.40 (7.01)		
Change from baseline in BDI-II	3.95 (4.91)	1.20 (8.04)	2.75 (-1.51 to 7.02)	0.1998
BAI, mean (SD)[b]				
Baseline	11.25 (6.17)	12.90 (12.13)		
Treatment, 1-4wk	5.95 (8.31)	8.25 (8.33)		
Change from baseline in BAI	3.95 (9.59)	5.85 (10.09)	0.65 (-3.84 to 5.15)	0.7715
MoCA, mean (SD)[b] MoCA total score				
Baseline	26.58 (2.87)	26.74 (2.60)		
Treatment, 1-4wk	27.71 (2.03)	27.16 (2.39)		
Change from baseline in MoCA	1.05 (1.27)	0.37 (1.26)	0.68 (-0.15 to 1.51)	0.1035
MoCA, Visuospatial and executive function				
Baseline	4.26 (1.37)	3.89 (1.37)		
Treatment, 1-4wk	4.68 (0.75)	3.84 (1.34)		
Change from baseline in MoCA	0.42 (0.77)	−0.05 (0.52)	0.47 (0.04 to 0.91)	0.0328
MoCA, Name recognition				
Baseline	2.89 (0.46)	2.89 (0.32)		
Treatment, 1-4wk	2.84 (0.50)	2.95 (0.23)		
Change from baseline in MoCA	−0.05 (0.23)	0.05 (0.23)	−0.11 (-0.26 to 0.05)	0.1659
MoCA, Attention				
Baseline	5.95 (0.23)	5.84 (0.37)		
Treatment, 1-4wk	5.95 (0.23)	5.89 (0.32)		
Change from baseline in MoCA	0 (0.33)	0.06 (0.52)	−0.05 (-0.34 to 0.24)	0.7141
MoCA, Language				
Baseline	2.37 (0.68)	2.63 (0.60)		
Treatment, 1-4wk	2.79 (0.18)	2.63 (0.60)		
Change from baseline in MoCA	0.42 (0.51)	0 (0.67)	0.42 (0.31 to 0.81)	0.0351
MoCA, Abstract				
Baseline	1.95 (0.23)	1.95 (0.23)		

Table 2 (*continued*)

Outcome Measure	Real Acupuncture group n = 20	Sham Acupuncture group n = 20		Between-group difference
		Value (95 % CI)		P value[a]
Treatment, 1-4wk	1.90 (0.32)	1.94 (0.23)		
Change from baseline in MoCA	−0.05 (0.23)	0 (0.33)	−0.05 (-0.24 to 0.14)	0.5743
MoCA, Delayed memory				
Baseline	3.21 (1.32)	3.58 (1.30)		
Treatment, 1-4wk	3.47 (1.39)	3.89 (1.15)		
Change from baseline in MoCA	0.26 (0.93)	0.32 (0.75)	−0.05 (-0.61to 0.50)	0.8491
MoCA, Orientation				
Baseline	5.89 (0.32)	5.95 (0.23)		
Treatment, 1-4wk	5.94(0.23)	5.95 (0.23)		
Change from baseline in MoCA	0.05 (0.23)	0 (0.33)	0.05 (-0.05 to 0.16)	0.3240
PSQI, mean (SD)[b]				
Baseline	6.75 (5.41)	6.85 (3.07)		
Treatment, 1-4wk	5.65 (2.64)	6.60 (2.98)		
Change from baseline in PSQI	1.10 (3.46)	0.25 (2.53)	0.85 (-1.09 to 2.79)	0.3811

Abbreviations: *SD* standard deviation; *CI* confidence interval; *VAS* visual analog scale; *MMDs* Monthly migraine days; *HIT-6* 6-item Headache Impact Test; *MSQ* Migraine-Specific Quality of Life Questionnaire; *BDI-II* Beck Depression Inventory-II; *BAI* Beck Anxiety Inventory; *MoCA* Montreal Cognitive Assessment; *PSQI* Pittsburgh Sleep Quality Index.

[a] All tests were two-sided. Statistical significance was set at $P < 0.05$.
[b] Analyzed using independent samples *t-test*.

computation, we created 6-mm radius spherical masks based on the peak coordinates involving right AMYG (peak MNI coordinates: 24, −2, 18), left INS (peak MNI coordinates: −34, 18, 4), left PFCventmed, (peak MNI coordinates: −2, 54, −10), left MOG (peak MNI coordinates −48, −68, 4), and right MCC (peak MNI coordinates:2, 20, 32) and combined them to generate a mask of all ROIs (Fig. S2). After obtaining the overlap of the masks and the original uniformity test map, we refined the five ROIs and constructed a mask of all five ROIs for the seed-to-voxel connectivity analysis.

3.4. FC results

Two-way repeated measure ANOVA was conducted on rsFC with factors' group (real and sham acupuncture) and time (pre- and post-treatment). After 4 weeks of treatment, when using AMYG as seed, no significant main effect was revealed, while a significant rsFC time-by-groups interaction effect was noted. The real acupuncture could increase the rsFC in the left middle temporal gyrus (MTG) (peak MNI coordinates: −45, −66, 15; cluster size: 18 voxels; cluster-corrected $P_{GRF} < 0.05$) compared to the sham acupuncture group (Fig. 4, Table 3). To investigate this significant interaction, post-hoc *t*-test was performed between the two groups at baseline and after 4 weeks of treatment. No significant effect was observed at baseline, but a simple effect of post-treatment in the left MTG (peak MNI coordinates: −48,

−63, 15; cluster size: 7 voxels; cluster-corrected $P_{GRF} < 0.05$) suggested that the interaction effect was driven by the difference between groups after 4 weeks of treatment.

When using MCC as seed, a significant main effect of treatment was noted in INS, bilateral precentral gyrus, bilateral middle cingulate cortex, left supplementary motor area, and right postcentral gyrus (Table S4). A significant rsFC time-by-groups interaction effect was observed in the right STG and left MTG. The real acupuncture increases the rsFC in the right STG (peak MNI coordinates: 66, −15, −9; cluster size: 12 voxels; cluster-corrected $P_{GRF} < 0.05$) and left MTG (peak MNI coordinates: −63, −9, −9; cluster size: 27 voxels; cluster-corrected $P_{GRF} < 0.05$) compared to the sham acupuncture group (Fig. 4, Table 3). To investigate this significant interaction, post-hoc *t*-test was performed between the two groups at baseline and 4 weeks of treatment. No significant simple effect was found at the baseline, a simple effect of post-treatment was noted in the left MTG (peak MNI coordinates: −63, −6, −12; cluster size: 6 voxels; cluster-corrected $P_{GRF} < 0.05$), suggesting that the interaction effect was driven by the difference between groups after 4 weeks of treatment.

Real acupuncture > sham acupuncture. Statistically significant effects were determined at a voxel-wise level of $P < 0.001$ and Gaussian random field cluster-corrected threshold of $P_{GRF} < 0.05$. Abbreviations: *AMYG* amygdala; *MCC* middle cingulate cortex; *MTG* middle temporal gyrus; *STG* superior temporal gyrus.

Moreover, no significant interaction-effect regions were revealed using the mask of all ROIs, left MOG, left INS, or left PFCventmed as seeds. However, when using INS as seed, a main effect of treatment was observed in the left superior frontal gyrus and right supplementary motor area (Table S4). When using PFCventmed as seed, a main effect of treatment was observed in the left Cerebellum_Crus2, right Cerebellum_Crus1, bilateral medial superior frontal gyrus, bilateral middle frontal gyrus, right middle temporal gyrus, right middle occipital gyrus, right precuneus, and left angular (Table S2).

Also, the migraine patients in the real acupuncture group showed an increased rsFC in the left cuneus with right MCC after acupuncture treatment (Fig. 4), while no significant rsFC region was detected in the sham acupuncture group.

3.5. Correlations results

Herein, we found an overlapping increase in the left MTG whenever using right AMYG or right MCC as seed. Thus, we extracted the average rsFC z-values of the overlapping region in the left MTG for the following analysis. Next, we computed a correlation coefficient between the extracted average z-values of the rsFC change and the clinical feature change (including MMDs, VAS, HIT-6, MSQ, BDI-II, BAI, PSQI, and MoCA) across all patients (post-treatment − pre-treatment) and observed that the increased rsFC z-value in the left MTG with the right AMYG seed was negatively associated with reduced MMDs (r = -0.333 $P_{uncorrected} = 0.0356$, $P_{Bonferroni-corrected} = 0.356$). Conversely, the increased rsFC z-value in the left MTG with right MCC was negatively associated with the increased MSQ-RP domain score (r = -0.483 $P_{uncorrected} = 0.0016$, $P_{Bonferroni-corrected} = 0.016$) and reduced HIT-6 score (r = -0.527$P_{uncorrected} = 0.0005$, $P_{Bonferroni-corrected} = 0.005$). The FC result was normally distributed (P > 0.05). The correlation between the reduced MMDs and increased rsFC z-value in the left MTG with the right AMYG seed did not survive after Bonferroni correction, but showed a significant trend. The results are shown in Fig. 5.

We also extracted the average rsFC z-values of the left MTG at the baseline to explore whether it could predict the treatment response. A hierarchical multiple regression analysis controlling for age, sex, and education was applied. Next, we observed a significantly decreased correlation between rsFC z-values in the left MTG at baseline and the MMDs change ($R^2 = 0.167 F (4, 35) = 1.756 P = 0.043$) when using the right AMYG as seed, proposing that the rsFC of right AMYG-left MTG has the potential to predict the treatment response. Moreover, no significant
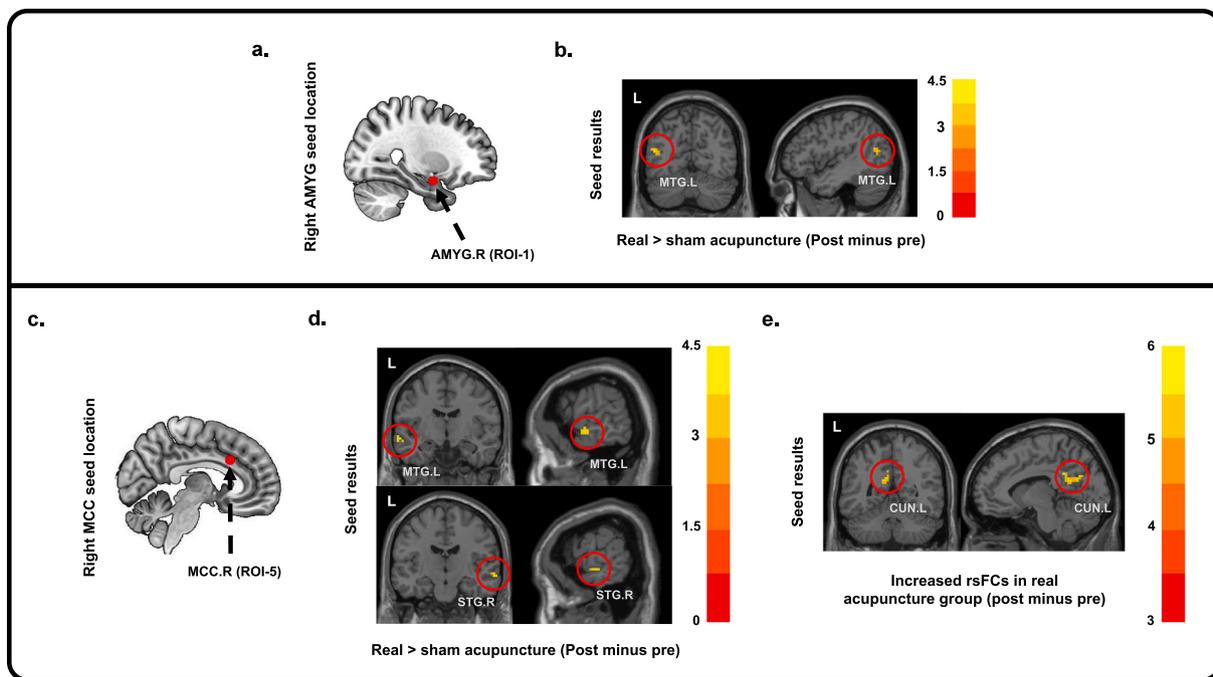
Fig. 4. (a) The location of the right AMYG (ROI-1) seed (marked in red). **(b)** A significant rsFC time-by-groups interaction effect was noted in the left MTG (post minus pre). **(c)** The location of the right MCC (ROI-5) seed (marked in red). **(d)** A significant rsFC time-by-groups interaction effect was noted in the left MTG and right STG (post minus pre). **(e)** The altered rsFC of right CUN in real acupuncture group after four weeks treatment. Abbreviations: ROI, region of interest; rsFC, resting state functional connectivity; MTG, middle temporal gyrus; MCC, middle cingulate cortex; STG, superior temporal gyrus; CUN, cuneus. (For interpretation of the references to colour in this figure legend, the reader is referred to the web version of this article.)

Table 3
Interaction effect between real and sham acupuncture group after four weeks treatment.

Seed	Brain regions	Cluster size	T peak	Peak coordinates		
Right AMYG	Left MTG	18	4.4692	−45	−66	15
Right MCC	Left MTG	27	4.1278	−63	−9	−9
	Right STG	12	4.1853	66	−15	−9

correlation was observed when using the right MCC as seed.

4. Discussion

The between-group differences were significant for MMDs, HIT-6, MSQ-RR, and MSQ-RP domains in favor of real acupuncture, reflecting improvement in the treatment effects on headache severity, headache impact, and HRQoL. Then, we aimed to examine the effects of acupuncture in regulating brain connectivity of key regions, selected using the *meta*-analysis on brain imaging studies of pain. The results were as follows: 1) After acupuncture treatment, migraine patients of the real acupuncture group showed significantly enhanced connectivity in the right AMYG/MCC-left MTG and right MCC-right STG compared to that of the sham acupuncture group; 2) Negative correlations were established between clinical effects and increased rsFC in the right AMYG/MCC-left MTG; 3) Baseline right AMYG-left MTG rsFC could predict the decrease in the MMDs after treatment. The current findings implied that acupuncture might concurrently regulate the rsFC of two pain modulation regions in the AMYG and MCC. The MTG and STG may be the key nodes linked to multisensory processing of pain modulation in migraine with acupuncture treatment.

4.1. Clinical outcomes

The current study reported the efficacy of acupuncture on the measures of headache severity (MMDs, VAS), headache impact (HIT-6),

HRQoL (MSQ), psychological profile (BDI-II, BAI), sleep quality (PSQI), and cognitive function (MoCA). The results indicated that the treatment effects of real acupuncture are sustained for 4 weeks on MMDs, HIT-6, and MSQ compared to sham acupuncture. By week 4, the between-group mean differences in the change in HIT-6 and MSQ-RP domain scores were greater than the between-group MIDs (HIT-6 MID = 2.3 points; MSQ-RP MID = 4.6, Table 2) (Coeytaux et al., 2006; Cole et al., 2009). Accordingly, real acupuncture produced statistically significant and clinically meaningful improvements in the headache impact and HRQoL that were sustained for 4 weeks. These findings were in line with the results of a systematic review investigating the efficacy of acupuncture for migraine prevention (Linde et al., 2016), which supported and extended the previous findings (Wang et al., 2011; Xu et al., 2020; Zhao et al., 2017).

4.2. Pain modulation-related ROI functions in context of migraine

In this study, we used the *meta*-analysis on brain imaging studies of pain to identify the five pain modulation-related key regions, including right AMYG, left INS, left PFCventmed, left MOG, and right MCC. The current study aimed to examine the effects of acupuncture in regulating brain connectivity of the abovementioned pain modulation-related key regions in migraine patients. When using right AMYG and right MCC as seeds, significantly brain connectivity was observed after real acupuncture compared to sham acupuncture.

Our literature search found that AMYG and MCC brain regions had been widely reported in migraine studies. AMYG is a crucial part of the limbic system and is well-known for emotional processing (Janak and Tye, 2015; Marek et al., 2013). Many neuroimaging studies have demonstrated that AMYG plays a key role in pain modulation (Bushnell et al., 2013; Simons et al., 2014; Thompson and Neugebauer, 2017) and pain perception (Raver et al., 2020). In experimental pain processing studies, AMYG activation has been observed in response to experimental noxious stimuli, such as mechanical compression, thermal stimulation, electrical stimulation, and capsaicin application (Simons et al., 2014). In
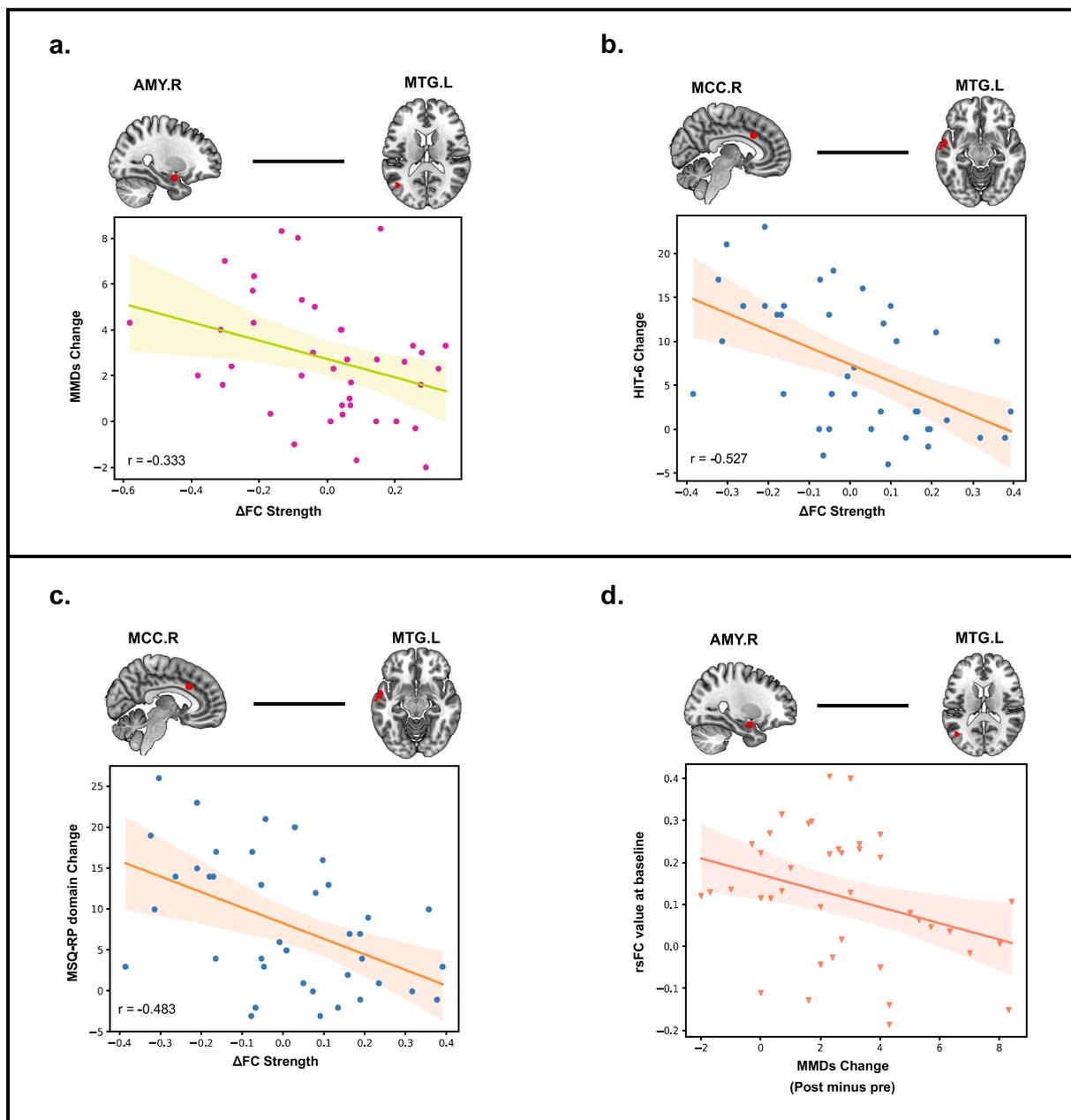
Fig. 5. (a) The significantly negatively correlation between rsFC change in left MTG with right AMYG and MMDs change across all MWoAs. **(b)** The significantly negatively correlation between rsFC change in left MTG with right MCC and HIT-6 change across all MWOAs. **(c)** The significantly negatively correlation between rsFC change in left MTG with right MCC and MSQ-RP domain change across all MWoAs. **(d)** Predicting the MMDs change with baseline average rsFC z-values in left MTG controlling for age, sex, and educational years. Abbreviations: MTG, middle temporal gyrus; AMYG, amygdala; MMDs, mean migraine days; MWoAs, migraine without aura; MCC, middle cingulate cortex; HIT-6, Headache Impact Test-6; MSQ-RP, Migraine-Specific Quality of Life Questionnaire-role preventive.

a structural MRI study, compared to healthy volunteers, the AMYG volumes fluctuated in MWoA patients and were correlated with headache frequency (Liu et al., 2017). Moreover, a significant change has been identified in a Granger causality analysis (GCA) of AMYG to other sensory cortical brain regions in MWoA, which indicates that AMYG contributes to the abnormalities in multisensory integration and pain modulation in migraine (Huang et al., 2021).

MCC is one of the key regions involved in the central executive network (CEN), implicated in the cognitive processes of pain modulation (Jiang et al., 2016). It is also a crucial part involved in the cortical mechanism of pain sensitization (Tan et al., 2017). Decreased MCC activity has been detected in migraineurs, and abnormal effective FC between the left MCC to right paracentral lobule is negatively correlated with the headache impact scores (Wei et al., 2020). A structural MRI

study showed reduced cortical thickness in the MCC in migraineurs (Hubbard et al., 2014). The above findings provided evidence that AMYG and MCC contribute to pain modulation in migraine.

4.3. Changes in brain connectivity linked to multisensory processing of pain modulation in migraine with acupuncture treatment

Importantly, we found that the left MTG was the overlapping brain region when using the right AMYG and right MCC as seeds after real acupuncture compared to sham acupuncture. A previous study confirmed that the MTG plays a critical role in multisensory information processing in migraine, especially for visual form. Both migraine with and migraine without aura patients display interictal impairments of the vision. The MTG is within the extrastriate visual cortex in the temporal

lobe. MTG contains predominant reciprocal connectivity with the visual regions V1–V4 as well as higher-order visual regions, such as the ventral intraparietal, superior temporal, and parieto-occipital cortex (Unger-leider and Desimone, 1986). The primary visual cortex and extrastriate visual cortex display altered excitability or sensitivity in migraineurs (Battelli et al., 2002). Another study suggested stronger activation of the left MTG in MWoA patients (Antal et al., 2011). Moreover, MTG presented decreased FC with left vlPAG in migraineurs than in healthy controls (Chen et al., 2017). Additionally, structural abnormality of the MTG was described previously in migraine (Granziera et al., 2006). The gray matter (GM) structure within the temporal lobes has been correlated with disease duration in migraineurs (Rocca et al., 2006). Inter-regional cortical thickness correlations of MTG and temporal pole can differentiate the migraine brain from the healthy brain (Schwedt et al., 2015a). Some studies indicated that MTG mainly participates in visual information processing and plays a crucial role in migraine pathophysiology, indicating that disrupted visual information processing may occur in migraine patients. Interestingly, a recent study showed that the decrease in the number of migraine days was related to the temporal gyrus's baseline GM volume, and the temporal gyrus demonstrated a longitudinal elevation in the GM volume in acupuncture treatment responders (Yang et al., 2020). Selected bilateral temporal lobe as ROI, Zou et al. indicated increased pairwise connectivity between the right temporal lobe and left anterior cingulate cortex, bilateral superior medial gyrus and right precuneus after acupuncture treatment(Zou et al., 2019). Increased connectivity in the MTG within the frontal and temporal lobes is seen following acupuncture treatment in migraine patients (Zhang et al., 2016). In this study, increased intrinsic connectivity within the MTG in migraine patients might provide a neuroanatomical basis for interpreting the real acupuncture mechanism.

Another main finding yielded is a significantly increased right STG rsFC when using the right MCC as seed after real acupuncture compared to sham acupuncture. During the interictal period, MWoA patients might still suffer hypersensitivity to multisensory stimuli. Several studies have confirmed that STG is also involved in increased multisensory processing in migraine, especially for auditory, visual, olfactory, and painful stimuli (Demarquay et al., 2008; Moulton et al., 2011; Schwedt, 2013). The STG is widely regarded as a critical component in multisensory perception and emotional regulation (Moerel et al., 2014; Schönwiesner and Zatorre, 2009; Yi et al., 2019), which is required for individual cognitive processes and adaptive behavior. Moreover, the STG belongs to the ventral stream of the visual pathway, effectuated as a link between auditory and visual processing, perception, and memory (Kravitz et al., 2013). A recent study found diminished ReHo value in right STG after acupuncture treatment, indicating emotional disorders in menstrual migraine without aura patients and the association with the acupuncture effects as well (Zhang et al., 2021). However, contrary results of an elevated ReHo value in STG and lowered in MTG were reported after acupuncture in a previous study (Zhao et al., 2014). In accordance with our findings, enhanced connectivity with the right STG and right precuneus was demonstrated following longitudinal acupuncture treatment(Li et al., 2017).

Strikingly, the real acupuncture treatment increased the rsFC within MTG and STG brain regions, which are both involved in multisensory processing in migraine, including visual, auditory, and language recognition. The patients in the real acupuncture group showed increased visuospatial and executive function scores and language of the MoCA scale compared to the sham acupuncture group (Table 2). An increased MTG and STG connectivity may represent the improved capability of multisensory processing after treatment.

In the present study, the clinical effects (MMDs, HIT-6, and MSQ-RP domain) of the acupuncture treatment were significantly and negatively associated with increased rsFC in the left MTG with right AMYG/MCC. In agreement with these findings, the current study suggested that migraine patients display decreased brain connectivity in the pain modulation and multisensory processing regions, which could be

normalized by acupuncture along with headache severity, headache impact, and HRQoL improvement. These findings might prompt the improvement in clinical outcomes. We also found a significant negative association between right AMYG- left MTG rsFC at baseline and MMD decline, indicating that baseline right AMYG- left MTG rsFC could predict the magnitude of acupuncture treatment effects.

Migraine can be regarded as the consequence of multisensory interactions between pain emotional modulation and pain cognitive processing (Huang et al., 2021). The feedback mechanism that suppresses sensory perception is malfunctioning, and the abnormal sensory signals are transmitted to the brain, resulting in conscious perception of nociception (Wei et al., 2019). Taken together, these findings suggested that plasticity change in the multisensory processing cortex of pain modulation might be implicated in the mechanism underlying the treatment effects of acupuncture for migraine prevention. After acupuncture treatment, the enhanced connectivity in the right AMYG/MCC-left MTG and right MCC-right STG might be associated with functional normalization in the pain modulation mechanisms and ameliorate repeated unpleasant multisensory burden in the long-term pain response.

4.4. Limitations

Nevertheless, the present study has several limitations. First, our study was carried out during a 4-week treatment phase. Therefore, the acupuncture intervention shown in fMRI represents only short-to-middle-term effects. Second, our study had a small sample size, necessitating additional studies with large sample sizes to confirm our findings. Third, we did not apply multimodal imaging techniques at baseline and after the treatment. The regulation of the regional brain dysfunction with only rs-FCs is inadequate to describe the pathological mechanisms of migraine with acupuncture treatment. Fourth, migraine can be investigated in both the ictal and interictal phases, and migraineurs in different phases and subtypes have evoked diverse brain functional outcomes. In the current study, migraine without aura patients underwent MRI scanning during the headache-free interval. The timing of the data collection should be considered when interpreting the fMRI study, and our study may only represent acupuncture actions on a specific subtype of migraine. Fifth, Neurosynth *meta*-analysis also has some limitations. Errors may arise during the automated extraction and synthesis of fMRI activation coordinates. However, several studies have been conducted to demonstrate the validity and sensitivity of Neurosynth-based *meta*-analysis, which might provide evidence in support of the method's application (Yarkoni et al., 2011). Sixth, because of the lack of healthy controls, we cannot provide the characteristics on migraine neuroimaging, and the comparisons on rsFC between our intervention and normal states.

5. Conclusion

In conclusion, we used the *meta*-analysis on brain imaging studies of pain to identify the five pain modulation-related key regions, including right AMYG, left INS, left PFCventmed, left MOG, and right MCC. The migraine patients of the real acupuncture group showed significantly enhanced connectivity in the right AMYG/MCC-left MTG and right MCC-right STG compared to the sham acupuncture group. A negative correlation was established between the clinical effects and increased rsFC in the right AMYG/MCC-left MTG. Acupuncture may concurrently regulate the rsFC of two pain modulation regions in the AMYG and MCC. The MTG and STG might be the key nodes linked to multisensory processing of pain modulation in migraine with acupuncture treatment. Our findings highlighted the acupuncture potential in migraine management as well as the mechanisms underlying the modulation effects.

CRediT authorship contribution statement

Lu Liu: Writing – original draft, Writing – review & editing, Formal

analysis, Visualization, Funding acquisition. **Tian-Li Lyu:** Writing – original draft, Formal analysis, Visualization. **Ming-Yang Fu:** Writing – original draft, Formal analysis, Visualization. **Lin-Peng Wang:** Conceptualization, Investigation, Writing – review & editing, Funding acquisition. **Ying Chen:** Investigation, Writing – review & editing. **Jia-Hui Hong:** Investigation, Writing – review & editing. **Qiu-Yi Chen:** Investigation, Writing – review & editing. **Yu-Pu Zhu:** Investigation, Writing – review & editing. **Zhong-Jian Tan:** Investigation, Writing – review & editing. **Da-Peng Liu:** Investigation, Writing – review & editing. **Zi-Wei Chen:** Investigation, Writing – review & editing. **Ya-Zhuo Kong:** Conceptualization, Writing – review & editing, Supervision, Methodology. **Bin Li:** Conceptualization, Writing – review & editing, Supervision, Methodology, Funding acquisition.

Declaration of Competing Interest

The authors declare that they have no known competing financial interests or personal relationships that could have appeared to influence the work reported in this paper.

Data availability

Data will be made available on request.

Appendix A. Supplementary data

Supplementary data to this article can be found online at https://doi.org/10.1016/j.nicl.2022.103168.

References

Antal, A., Polania, R., Saller, K., Morawetz, C., Schmidt-Samoa, C., Baudewig, J., Paulus, W., Dechent, P., 2011. Differential activation of the middle-temporal complex to visual stimulation in migraineurs. Cephalalgia 31, 338–345.

Ashina, M., Buse, D.C., Ashina, H., Pozo-Rosich, P., Peres, M.F.P., Lee, M.J., Terwindt, G. M., Halker Singh, R., Tassorelli, C., Do, T.P., Mitsikostas, D.D., Dodick, D.W., 2021a. Migraine: integrated approaches to clinical management and emerging treatments. Lancet 397, 1505–1518.

Ashina, M., Katsarava, Z., Do, T.P., Buse, D.C., Pozo-Rosich, P., Özge, A., Krymchantowski, A.V., Lebedeva, E.R., Ravishankar, K., Yu, S., Sacco, S., Ashina, S., Younis, S., Steiner, T.J., Lipton, R.B., 2021b. Migraine: epidemiology and systems of care. Lancet 397, 1485–1495.

Battelli, L., Black, K.R., Wray, S.H., 2002. Transcranial magnetic stimulation of visual area V5 in migraine. Neurology 58, 1066–1069.

Beck, A.T., Epstein, N., Brown, G., Steer, R.A., 1988. An inventory for measuring clinical anxiety: Psychometric properties. Journal of Consulting and Clinical Psychology 56, 893–897.

Beck, A.T., Steer, R.A., Ball, R., Ranieri, W., 1996a. Comparison of Beck Depression Inventories -IA and -II in psychiatric outpatients. J Pers Assess 67, 588–597.

Beck, A.T., Steer, R.A., Brown, G.K., 1996b. Beck depression inventory-II. Psychological Corporation, San Antonio.

Bushnell, M.C., Ceko, M., Low, L.A., 2013. Cognitive and emotional control of pain and its disruption in chronic pain. Nat Rev Neurosci 14, 502–511.

Buysse, D.J., Reynolds 3rd, C.F., Monk, T.H., Berman, S.R., Kupfer, D.J., 1989. The Pittsburgh Sleep Quality Index: a new instrument for psychiatric practice and research. Psychiatry Res 28, 193–213.

2013a. 2013a. The International Classification of Headache Disorders, 3rd edition (beta version). Cephalalgia 33, 629-808.

2018c. 2018c. Headache Classification Committee of the International Headache Society (IHS) The International Classification of Headache Disorders, 3rd edition. Cephalalgia 38, 1-211.

Chang, C.M., Yang, C.P., Yang, C.C., Shih, P.H., Wang, S.J., 2021. Evidence of Potential Mechanisms of Acupuncture from Functional MRI Data for Migraine Prophylaxis. Curr Pain Headache Rep 25, 49.

Chen, Z., Chen, X., Liu, M., Liu, S., Ma, L., Yu, S., 2017. Disrupted functional connectivity of periaqueductal gray subregions in episodic migraine. J Headache Pain 18, 36.

Coeytaux, R.R., Kaufman, J.S., Chao, R., Mann, J.D., Devellis, R.F., 2006. Four methods of estimating the minimal important difference score were compared to establish a clinically significant change in Headache Impact Test. J Clin Epidemiol 59, 374–380.

Cole, J.C., Lin, P., Rupnow, M.F., 2009. Minimal important differences in the Migraine-Specific Quality of Life Questionnaire (MSQ) version. Cephalalgia 29, 1180–1187.

Cole, D.M., Smith, S.M., Beckmann, C.F., 2010. Advances and pitfalls in the analysis and interpretation of resting-state FMRI data. Front Syst Neurosci 4, 8.

Demarquay, G., Royet, J.P., Mick, G., Ryvlin, P., 2008. Olfactory hypersensitivity in migraineurs: a H(2)(15)O-PET study. Cephalalgia 28, 1069–1080.

Dowson, A.J., 2001. Assessing the impact of migraine. Curr Med Res Opin 17, 298–309.

Eigenbrodt, A.K., Ashina, H., Khan, S., Diener, H.C., Mitsikostas, D.D., Sinclair, A.J., Pozo-Rosich, P., Martelletti, P., Ducros, A., Lantéri-Minet, M., Braschinsky, M., Del Rio, M.S., Daniel, O., Özge, A., Mammadbayli, A., Arons, M., Skorobogatykh, K., Romanenko, V., Terwindt, G.M., Paemeleire, K., Sacco, S., Reuter, U., Lampl, C., Schytz, H.W., Katsarava, Z., Steiner, T.J., Ashina, M., 2021. Diagnosis and management of migraine in ten steps. Nat Rev Neurol 17, 501–514.

Frances, A., First, M.B., Pincus, H.A., 1995. DSM-IV guidebook. American Psychiatric Association.

2018b. 2018b. Global, regional, and national incidence, prevalence, and years lived with disability for 354 diseases and injuries for 195 countries and territories, 1990-2017: a systematic analysis for the Global Burden of Disease Study 2017. Lancet 392, 1789-1858.

2019 2019. Global, regional, and national burden of neurological disorders, 1990-2016: a systematic analysis for the Global Burden of Disease Study 2016. Lancet Neurol 18, 459-480.

Granziera, C., DaSilva, A.F., Snyder, J., Tuch, D.S., Hadjikhani, N., 2006. Anatomical alterations of the visual motion processing network in migraine with and without aura. PLoS Med 3, e402.

Hepp, Z., Dodick, D.W., Varon, S.F., Gillard, P., Hansen, R.N., Devine, E.B., 2015. Adherence to oral migraine-preventive medications among patients with chronic migraine. Cephalalgia 35, 478–488.

Huang, X., Zhang, D., Wang, P., Mao, C., Miao, Z., Liu, C., Xu, C., Yin, X., Wu, X., 2021. Altered amygdala effective connectivity in migraine without aura: evidence from resting-state fMRI with Granger causality analysis. J Headache Pain 22, 25.

Hubbard, C.S., Khan, S.A., Keaser, M.L., Mathur, V.A., Goyal, M., Seminowicz, D.A., 2014. Altered Brain Structure and Function Correlate with Disease Severity and Pain Catastrophizing in Migraine Patients. eNeuro 1, e20 14.

2013b. 2013b. World Medical Association Declaration of Helsinki: ethical principles for medical research involving human subjects. Jama 310, 2191-2194.

Janak, P.H., Tye, K.M., 2015. From circuits to behaviour in the amygdala. Nature 517, 284–292.

Jhingran, P., Davis, S.M., LaVange, L.M., Miller, D.W., Helms, R.W., 1998a. MSQ: Migraine-Specific Quality-of-Life Questionnaire. Further investigation of the factor structure. Pharmacoeconomics 13, 707–717.

Jhingran, P., Osterhaus, J.T., Miller, D.W., Lee, J.T., Kirchdoerfer, L., 1998b. Development and validation of the Migraine-Specific Quality of Life Questionnaire. Headache 38, 295–302.

Jiang, Y., Oathes, D., Hush, J., Darnall, B., Charvat, M., Mackey, S., Etkin, A., 2016. Perturbed connectivity of the amygdala and its subregions with the central executive and default mode networks in chronic pain. Pain 157, 1970–1978.

Kosinski, M., Bayliss, M.S., Bjorner, J.B., Ware Jr., J.E., Garber, W.H., Batenhorst, A., Cady, R., Dahlof, C.G., Dowson, A., Tepper, S., 2003. A six-item short-form survey for measuring headache impact: the HIT-6. Qual Life Res 12, 963–974.

Kravitz, D.J., Saleem, K.S., Baker, C.I., Ungerleider, L.G., Mishkin, M., 2013. The ventral visual pathway: an expanded neural framework for the processing of object quality. Trends Cogn Sci 17, 26–49.

Lee, M.J., Park, B.Y., Cho, S., Kim, S.T., Park, H., Chung, C.S., 2019. Increased connectivity of pain matrix in chronic migraine: a resting-state functional MRI study. J Headache Pain 20, 29.

Li, Z., Lan, L., Zeng, F., Makris, N., Hwang, J., Guo, T., Wu, F., Gao, Y., Dong, M., Liu, M., Yang, J., Li, Y., Gong, Q., Sun, S., Liang, F., Kong, J., 2017. The altered right frontoparietal network functional connectivity in migraine and the modulation effect of treatment. Cephalalgia 37, 161–176.

Li, Y., Liang, F., Yang, X., Tian, X., Yan, J., Sun, G., Chang, X., Tang, Y., Ma, T., Zhou, L., Lan, L., Yao, W., Zou, R., 2009. Acupuncture for treating acute attacks of migraine: a randomized controlled trial. Headache 49, 805–816.

Li, Y., Zheng, H., Witt, C.M., Roll, S., Yu, S.G., Yan, J., Sun, G.J., Zhao, L., Huang, W.J., Chang, X.R., Zhang, H.X., Wang, D.J., Lan, L., Zou, R., Liang, F.R., 2012. Acupuncture for migraine prophylaxis: a randomized controlled trial. Cmaj 184, 401–410.

Linde, K., Allais, G., Brinkhaus, B., Fei, Y., Mehring, M., Vertosick, E.A., Vickers, A., White, A.R., 2016. Acupuncture for the prevention of episodic migraine. Cochrane Database Syst Rev 2016, Cd001218.

Liu, H.Y., Chou, K.H., Lee, P.L., Fuh, J.L., Niddam, D.M., Lai, K.L., Hsiao, F.J., Lin, Y.Y., Chen, W.T., Wang, S.J., Lin, C.P., 2017. Hippocampus and amygdala volume in relation to migraine frequency and prognosis. Cephalalgia 37, 1329–1336.

Liu, L., Tian, T., Li, X., Wang, Y., Xu, T., Ni, X., Li, X., He, Z., Gao, S., Sun, M., Liang, F., Zhao, L., 2021. Revealing the Neural Mechanism Underlying the Effects of Acupuncture on Migraine: A Systematic Review. Front Neurosci 15, 674852.

Marek, R., Strobel, C., Bredy, T.W., Sah, P., 2013. The amygdala and medial prefrontal cortex: partners in the fear circuit. J Physiol 591, 2381–2391.

Moerel, M., De Martino, F., Formisano, E., 2014. An anatomical and functional topography of human auditory cortical areas. Front Neurosci 8, 225.

Moulton, E.A., Becerra, L., Maleki, N., Pendse, G., Tully, S., Hargreaves, R., Burstein, R., Borsook, D., 2011. Painful heat reveals hyperexcitability of the temporal pole in interictal and ictal migraine States. Cereb Cortex 21, 435–448.

Nasreddine, Z.S., Phillips, N.A., Bédirian, V., Charbonneau, S., Whitehead, V., Collin, I., Cummings, J.L., Chertkow, H., 2005. The Montreal Cognitive Assessment, MoCA: a brief screening tool for mild cognitive impairment. J Am Geriatr Soc 53, 695–699.

2018a 2018a. Global, regional, and national burden of migraine and tension-type headache, 1990-2016: a systematic analysis for the Global Burden of Disease Study 2016. Lancet Neurol 17, 954-976.

O'Driscoll, C., Shaikh, M., 2017. Cross-Cultural Applicability of the Montreal Cognitive Assessment (MoCA): A Systematic Review. J Alzheimers Dis 58, 789–801.

Raver, C., Uddin, O., Ji, Y., Li, Y., Cramer, N., Jenne, C., Morales, M., Masri, R., Keller, A., 2020. An Amygdalo-Parabrachial Pathway Regulates Pain Perception and Chronic Pain. J Neurosci 40, 3424–3442.

Region, W.H.O.W.P., 2010. WHO standard acupuncture point locations in the Western Pacific Region. People's Medical Publishing House, Beijing.

Rocca, M.A., Ceccarelli, A., Falini, A., Colombo, B., Tortorella, P., Bernasconi, L., Comi, G., Scotti, G., Filippi, M., 2006. Brain gray matter changes in migraine patients with T2-visible lesions: a 3-T MRI study. Stroke 37, 1765–1770.

Ruscheweyh, R., Pereira, D., Hasenbring, M.I., Straube, A., 2019. Pain-related avoidance and endurance behaviour in migraine: an observational study. J Headache Pain 20, 9.

Russell, M.B., Rasmussen, B.K., Brennum, J., Iversen, H.K., Jensen, R.A., Olesen, J., 1992. Presentation of a new instrument: the diagnostic headache diary. Cephalalgia 12, 369–374.

Santangelo, G., Russo, A., Trojano, L., Falco, F., Marcuccio, L., Siciliano, M., Conte, F., Garramone, F., Tessitore, A., Tedeschi, G., 2016. Cognitive dysfunctions and psychological symptoms in migraine without aura: a cross-sectional study. J Headache Pain 17, 76.

Schönwiesner, M., Zatorre, R.J., 2009. Spectro-temporal modulation transfer function of single voxels in the human auditory cortex measured with high-resolution fMRI. Proc Natl Acad Sci U S A 106, 14611–14616.

Schwedt, T.J., 2013. Multisensory integration in migraine. Curr Opin Neurol 26, 248–253.

Schwedt, T.J., Berisha, V., Chong, C.D., 2015a. Temporal lobe cortical thickness correlations differentiate the migraine brain from the healthy brain. PLoS One 10, e0116687.

Schwedt, T.J., Chiang, C.C., Chong, C.D., Dodick, D.W., 2015b. Functional MRI of migraine. Lancet Neurol 14, 81–91.

Simons, L.E., Moulton, E.A., Linnman, C., Carpino, E., Becerra, L., Borsook, D., 2014. The human amygdala and pain: evidence from neuroimaging. Hum Brain Mapp 35, 527–538.

Singh, J., Joshi, A., Gupta, A., Mitra, A., Kumar Rai, N., 2020. Exploratory study to understand association of emotional comorbidities and sleep with migraine. Int J Neurosci 1–9.

Skorobogatykh, K., van Hoogstraten, W.S., Degan, D., Prischepa, A., Savitskaya, A., Ileen, B.M., Bentivegna, E., Skiba, I., D'Acunto, L., Ferri, L., Sacco, S., Hansen, J.M.,

Amin, F.M., 2019. Functional connectivity studies in migraine: what have we learned? J Headache Pain 20, 108.

Stanyer, E.C., Creeney, H., Nesbitt, A.D., Holland, P.R., Hoffmann, J., 2021. Subjective Sleep Quality and Sleep Architecture in Patients With Migraine: A Meta-analysis. Neurology 97, e1620 e1631.

Steer, R.A., Ball, R., Ranieri, W.F., Beck, A.T., 1999. Dimensions of the Beck Depression Inventory-II in clinically depressed outpatients. J Clin Psychol 55, 117–128.

Tan, L.L., Pelzer, P., Heinl, C., Tang, W., Gangadharan, V., Flor, H., Sprengel, R., Kuner, T., Kuner, R., 2017. A pathway from midcingulate cortex to posterior insula gates nociceptive hypersensitivity. Nat Neurosci 20, 1591–1601.

Thompson, J.M., Neugebauer, V., 2017. Amygdala Plasticity and Pain. Pain Res Manag 2017, 8296501.

Tian, Z., Guo, Y., Yin, T., Xiao, Q., Ha, G., Chen, J., Wang, S., Lan, L., Zeng, F., 2021. Acupuncture Modulation Effect on Pain Processing Patterns in Patients With Migraine Without Aura. Front Neurosci 15, 729218.

Ungerleider, L.G., Desimone, R., 1986. Cortical connections of visual area MT in the macaque. J Comp Neurol 248, 190–222.

Wang, L.P., Zhang, X.Z., Guo, J., Liu, H.L., Zhang, Y., Liu, C.Z., Yi, J.H., Wang, L.P., Zhao, J.P., Li, S.S., 2011. Efficacy of acupuncture for migraine prophylaxis: a single-blinded, double-dummy, randomized controlled trial. Pain 152, 1864–1871.

Wei, H.L., Zhou, X., Chen, Y.C., Yu, Y.S., Guo, X., Zhou, G.P., Zhou, Q.Q., Qu, L.J., Yin, X., Li, J., Zhang, H., 2019. Impaired intrinsic functional connectivity between the thalamus and visual cortex in migraine without aura. J Headache Pain 20, 116.

Wei, H.L., Chen, J., Chen, Y.C., Yu, Y.S., Guo, X., Zhou, G.P., Zhou, Q.Q., He, Z.Z., Yang, L., Yin, X., Li, J., Zhang, H., 2020. Impaired effective functional connectivity of the sensorimotor network in interictal episodic migraineurs without aura. J Headache Pain 21, 111.

Wei, X.Y., Luo, S.L., Chen, H., Liu, S.S., Gong, Z.G., Zhan, S.H., 2022. Functional connectivity changes during migraine treatment with electroacupuncture at Shuaigu (GB8). J Integr Med 20, 237–243.

Xu, S., Yu, L., Luo, X., Wang, M., Chen, G., Zhang, Q., Liu, W., Zhou, Z., Song, J., Jing, H., Huang, G., Liang, F., Wang, H., Wang, W., 2020. Manual acupuncture versus sham acupuncture and usual care for prophylaxis of episodic migraine without aura: multicentre, randomised clinical trial. Bmj 368, m697.

Yang, X.J., Liu, L., Xu, Z.L., Zhang, Y.J., Liu, D.P., Fishers, M., Zhang, L., Sun, J.B., Liu, P., Zeng, X., Wang, L.P., Qin, W., 2020. Baseline Brain Gray Matter Volume as a Predictor of Acupuncture Outcome in Treating Migraine. Front Neurol 11, 111.

Yarkoni, T., Poldrack, R.A., Nichols, T.E., Van Essen, D.C., Wager, T.D., 2011. Large-scale automated synthesis of human functional neuroimaging data. Nat Methods 8, 665–670.

Yi, H.G., Leonard, M.K., Chang, E.F., 2019. The Encoding of Speech Sounds in the Superior Temporal Gyrus. Neuron 102, 1096–1110.

Zhang, Y., Li, K.S., Liu, H.W., Fu, C.H., Chen, S., Tan, Z.J., Ren, Y., 2016. Acupuncture treatment modulates the resting-state functional connectivity of brain regions in migraine patients without aura. Chin J Integr Med 22, 293–301.

Zhang, Y., Wang, Z., Du, J., Liu, J., Xu, T., Wang, X., Sun, M., Wen, Y., Li, D., Liao, H., Zhao, Y., Zhao, L., 2021. Regulatory Effects of Acupuncture on Emotional Disorders in Patients With Menstrual Migraine Without Aura: A Resting-State fMRI Study. Front Neurosci 15, 726505.

Zhao, L., Liu, J., Zhang, F., Dong, X., Peng, Y., Qin, W., Wu, F., Li, Y., Yuan, K., von Deneen, K.M., Gong, Q., Tang, Z., Liang, F., 2014. Effects of long-term acupuncture treatment on resting-state brain activity in migraine patients: a randomized controlled trial on active acupoints and inactive acupoints. PLoS One 9, e99538.

Zhao, L., Chen, J., Li, Y., Sun, X., Chang, X., Zheng, H., Gong, B., Huang, Y., Yang, M., Wu, X., Li, X., Liang, F., 2017. The Long-term Effect of Acupuncture for Migraine Prophylaxis: A Randomized Clinical Trial. JAMA Intern Med 177, 508–515.

Zou, Y., Tang, W., Li, X., Xu, M., Li, J., 2019. Acupuncture Reversible Effects on Altered Default Mode Network of Chronic Migraine Accompanied with Clinical Symptom Relief. Neural Plast 2019, 5047463.